

NUMERICAL MODEL TO EVALUATE VARIATIONS OF STRAIN RATES DURING CONVENTIONAL OEDOMETER TESTS FOR CRS CONSOLIDATION PRACTICE

Abderrahmane Henniche^{1*}

ABSTRACT

The constant rate of strain (CRS) consolidation test can produce reliable results if an adequate strain rate is applied. Many criteria have been developed to select appropriate strain rates for the CRS consolidation test. Mesri and Feng recommended applying strain rates in a CRS consolidation test that could be 10 times greater than the end-of-primary strain rate (r_{cop}) evaluated during a conventional oedometer test. In this study, a numerical model was developed to evaluate the primary consolidation strain rates during a conventional oedometer test. The results obtained using the numerical model indicate that the predicted strain rates take large values at the beginning of the test and very small values at the end of the primary consolidation stage. Moreover, the strain rates depend on the load increment ratio adopted during the conventional oedometer test and rise by increasing the applied loads. The experimental strain rate variations during the primary consolidation of conventional oedometer tests found in the literature were compared with the predicted strain rate variations obtained by simulating the same tests with the numerical model, which indicated good agreement. The comparison also indicated that the end-of-primary strain rate evaluated from the experimental tests generally corresponded to the strain rate estimated by the numerical model, at an average degree of consolidation of approximately 99%. The strain rate obtained of $U_{avg} = 99\%$ could subsequently be used to give an approximate estimation of the appropriate strain rates to apply when using the CRS test with normally consolidated soils.

Key words: CRS test, conventional oedometer test, strain rate, numerical model, consolidation.

1. INTRODUCTION

The constant rate of strain (CRS) consolidation test has become frequently used in practice in recent decades. The CRS consolidation test presents many advantages over the conventional oedometer test, particularly its generation of continuous responses and shorter testing time (Hefu and Patrick 2016). However, the consolidation parameters evaluated from measured responses of the CRS consolidation test depend on the strain rate applied (Smith and Wahls 1969; Vaid *et al.* 1979; Leroueil *et al.* 1985; Sheahan and Watters 1997; Moriwaki and Umehara 2003; Adams 2011). Different criteria have been developed to select appropriate strain rates for the CRS consolidation test, including essentially the relative pressure criterion R_u (Smith and Wahls 1969; Wissa *et al.* 1971; Sheahan and Watters 1997), liquid limit criterion w_l (Gorman *et al.* 1978) and standarized strain rate criterion β (Lee 1981; Lee *et al.* 1993; Kassim *et al.* 2016). The most frequently used criterion requires the relative pressure values developed during the CRS test to be kept at less than a preset value that generally equals 15% (Mieussens *et al.* 1985; ASTM standard 2006; ASTM standard 2012). Another important criterion recommended by other authors (Mesri and Feng 1992; Almeida *et al.* 1995; Feng 2010) consists of estimating the appropriate strain rates for the CRS test from the parallelism between the consolidation conditions imposed in the conventional oedometer test and the CRS test. The convenient

Manuscript received January 31, 2023; revised March 30, 2023; accepted April 24, 2023.

¹*Assistant Professor (corresponding author), Department of civil engineering, Morsli Abdellah University Center, Tipaza, Algeria (e-mail: henabdhrhmne@gmail.com).

use of this criterion for a particular soil requires several conventional oedometer tests to be conducted and the appropriate end-of-primary conditions to be evaluated, particularly the strain rates. The purpose of this work was to develop a numerical model for estimating end-of-primary consolidation strain rates (r_{cop}) from conventional oedometer tests. Therefore, based on an empirical correlation between the consolidation characteristics and index properties of a given soil, the predicted end-of-primary consolidation strain rates could be used to provide an approximate estimation of the appropriate strain rates for a CRS consolidation test. In the absence of laboratory data concerning consolidation tests, using this numerical model in practice will avoid the need to conduct several conventional oedometer tests to obtain the proper end-of-primary consolidation strain rate.

2. MODEL DESCRIPTION

In general, Terzaghi's classic theory of consolidation is the most frequently used way of estimating the consolidation evolution with time of clayey soils. This theory was developed for small strain conditions, and it considers that the values of the coefficient of consolidation c_v and the coefficient of compressibility m_s are essentially constant, that soil particles and pore fluid are incompressible, and that Darcy's law is valid. Based on these assumptions, Terzaghi developed a one-dimensional consolidation equation:

$$c_v \frac{\partial^2 u}{\partial z^2} = \frac{\partial u}{\partial t} \quad (1)$$

where c_v is the coefficient of the consolidation of soil, and u is the excess pore water pressure generated at a vertical depth z of the soil sample and at time t during the consolidation process.

Equation (1) can be solved using the finite differences approach (Das 2008), with the two sides of this equation written as follows:

$$\frac{\partial^2 u}{\partial z^2} = \frac{1}{(\Delta z)^2} (u_{z+\Delta z,t} + u_{z-\Delta z,t} - 2u_{z,t}) \quad (2)$$

and

$$\frac{\partial u}{\partial t} = \frac{1}{\Delta t} (u_{z,t+\Delta t} - u_{z,t}) \quad (3)$$

If the soil sample is divided into n elements, the thickness of each soil element can be given as:

$$\Delta z = H / n \quad (4)$$

where H is the sample height that is considered constant until the end of the consolidation process, and Δt is the time step.

Substituting Eqs. (2) and (3) in Eq. (1), gives:

$$u_{z,t+\Delta t} = \frac{c_v \cdot \Delta t}{(\Delta z)^2} (u_{z+\Delta z,t} + u_{z-\Delta z,t} - 2u_{z,t}) + u_{z,t} \quad (5)$$

where $u_{z,t+\Delta t}$ and $u_{z,t}$ are the pore water pressure values at depth z and at times $t + \Delta t$ and t , respectively. $u_{z+\Delta z,t}$ and $u_{z-\Delta z,t}$ are the pore water pressure values at time t and at depths $z + \Delta z$ and $z - \Delta z$, respectively.

If the base of the sample ($z = H$) is undrained, we take ($u_{z+\Delta z,t} = u_{z-\Delta z,t}$), and Eq. (5) becomes:

$$u_{z,t+\Delta t} = \frac{c_v \cdot \Delta t}{(\Delta z)^2} (2u_{z-\Delta z,t} - 2u_{z,t}) + u_{z,t} \quad (6)$$

To assure the convergence of Eqs. (5) and (6), the values of Δt and Δz must be chosen such that:

$$\frac{c_v \cdot \Delta t}{(\Delta z)^2} < 0.5 \quad (7)$$

For conventional oedometer test, Eqs. (5) to (7) are used during each load increment. The constant applied load (σ_v), the void ratio e , and the sample height H must be evaluated at the beginning of each load increment:

$$\sigma_{v,i+1} = (1 + LIR) \cdot \sigma_{v,i} \quad (8)$$

where $\sigma_{v,i+1}$ and $\sigma_{v,i}$ are the values of the applied loads during the $i+1^{th}$ and i^{th} load increments, respectively. LIR is the load increment ratio adopted during the conventional oedometer test.

$$e_{i+1} = e_i - C_c \cdot \log(\sigma_{v,i+1} / \sigma_{v,i}) \quad (9)$$

where C_c is the compression index of the soil. e_{i+1} and e_i are the initial void ratio values at the beginning of the $i+1^{th}$ and i^{th} load increments, respectively.

$$H_{i+1} = H_i \cdot \left(1 - \frac{e_i - e_{i+1}}{1 + e_i}\right) \quad (10)$$

where H_{i+1} and H_i are the initial sample height values at the beginning of the $i+1^{th}$ and i^{th} load increments, respectively.

At the beginning of each load increment: $(u_{z,0})_i = \sigma_{v,i}$, and at the drained faces of the sample: $(\partial u / \partial z)_i = 0$.

Based on previous equations, the numerical model was developed to predict the strain rate variations of the primary consolidation phase during each load increment of the conventional oedometer test. The inputs of the model include the following:

- The initial height of the sample, H_0 .
- The initial void ratio of the sample, e_0 .
- The initial effective stress σ'_{v0} that corresponds to the initial void ratio e_0 . It is taken as the intersection between the extended virgin compression line, obtained from a compression curve of the soil, and the initial void ratio value e_0 .
- The coefficient of consolidation c_v values, which vary with the applied loads during the test. During each load increment, the value of c_v is considered constant.
- The compression index C_c value deduced from the compression curve of the soil.
- The values of the load increment ratio adopted during the conventional oedometer test.
- The number of soil sample elements n ($20 \leq n \leq 100$).

To assess the accuracy of the numerical model by comparing the experimental strain rates with the predicted strain rates, the inputs of the model must be taken from the experimental conventional oedometer tests. However, when using the model to estimate an approximate end-of-primary strain rate (r_{cop}) for normally consolidated soils, the coefficient of consolidation c_v and the compression index C_c can be obtained through empirical correlations with the index properties of the tested soil, such as the liquid limit, plasticity index, and shrinkage index (Terzaghi and Peck 1967; Wroth and Wood 1978; Sridharan and Nagaraj 2004; Vinod and Bindu 2010; Tiwari and Ajmera 2012; Nesamatha and Arumairaj 2015; Rashed et al 2017; Kaveh et Şirin 2022). Most studies indicate that the coefficient of consolidation c_v and the compression index C_c have good correlations with the liquid limit LL, but the coefficient of consolidation is best correlated with the plasticity index PI or the shrinkage index IS.

For normally consolidated soils, the U.S. Navy's (1971) approximate correlation (Fig. 1) can be used to estimate a constant value of the coefficient of consolidation c_v from the liquid limit LL, while the equation developed by Terzaghi and Peck (1967) can be used to estimate the compression index C_c from the liquid limit LL:

$$C_c = 0.009 (LL - 10) \quad (11)$$

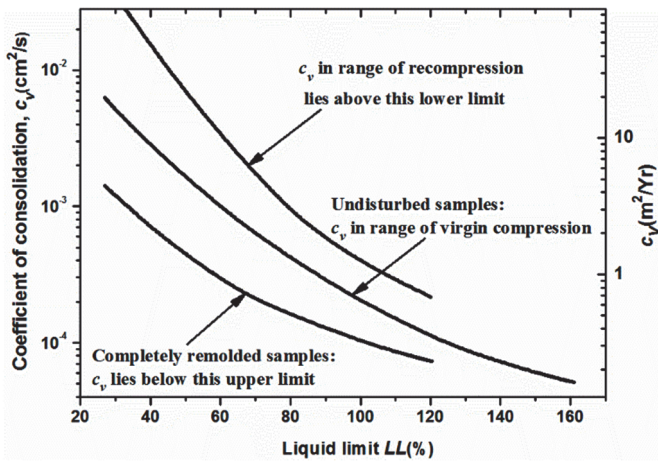


Fig. 1 Approximate correlation between coefficient of consolidation c_v and liquid limit LL (U.S. NAVY 1971)

During each load increment i , once the pore water pressure distribution has been evaluated along the soil sample at any time t using Eqs. (5) and (6), the average pore water pressure $u_{\text{avg}}(t)_i$ and the average degree of consolidation $U_{\text{avg}}(t)_i$ can be evaluated at the same time t :

$$u_{\text{avg}}(t)_i = \frac{1}{H} \int_0^H (u_{z,t})_i \cdot dz \quad (12)$$

$$U_{\text{avg}}(t)_i = 1 - \frac{u_{\text{avg}}(t)_i}{\sigma_{v,i}} \quad (13)$$

The total settlement of the sample is estimated at the end of each load increment using Eq. (10), and the sample settlement at any time during each load increment i is evaluated using the following equation:

$$S(t)_i = U_{\text{avg}}(t)_i \cdot (H_{i+1} - H_i) \quad (14)$$

The strain rate at a given average degree of consolidation U_{avg} during the load increment i is evaluated using the following equation:

$$r(t + \Delta t)_i = \frac{s(t + \Delta t)_i - s(t)_i}{\Delta t \cdot H_i} \quad (15)$$

During each load increment, calculations are stopped when the average degree of consolidation exceeds 99%. Besides, calculations of all conventional oedometer tests are stopped when a specified value of applied load $\sigma_{v,\text{max}}$ is exceeded ($\sigma_v > \sigma_{v,\text{max}}$) or when the average deformation of the sample reaches a fixed value ε_{max} .

3. MODEL RESULTS

To illustrate the fundamental results of the numerical model, a soil sample characterized by the following properties was taken as an example: coefficient of consolidation $c_v = 0.06 \text{ cm}^2/\text{min}$,

compression index $C_c = 0.45$, initial void ratio $e_0 = 1.2$ and initial height of sample $H_0 = 20 \text{ mm}$. Figure 2 shows the pore water pressure distribution along the soil sample under a constant load of 100 kPa at different loading times (1, 2, 3, 5, 7, 10, 15, 20, and 30 min), when the soil sample was drained at both the top and the bottom.

Figure 3 illustrates the variations of the average pore water pressure and average degree of consolidation under the same load and at the same loading times. Figure 4 shows the variations of predicted strain rates with the numerical model at the same times of loading for two different values of load increment ratio (0.5 and 1). Note that these values correspond to preceding applied loads of 67 kPa and 50 kPa, respectively. It's observed for each load increment ratio that the predicted strain rates decrease from greater values at the beginning of the load increment to small values at the end (especially for U_{avg} values greater than 95%). It's also observed that at the same time the predicted strain rate for the load increment ratio of 1 is greater than that estimated for the load increment ratio of 0.5, although the difference is not significant in particular at the end of primary consolidation stage.

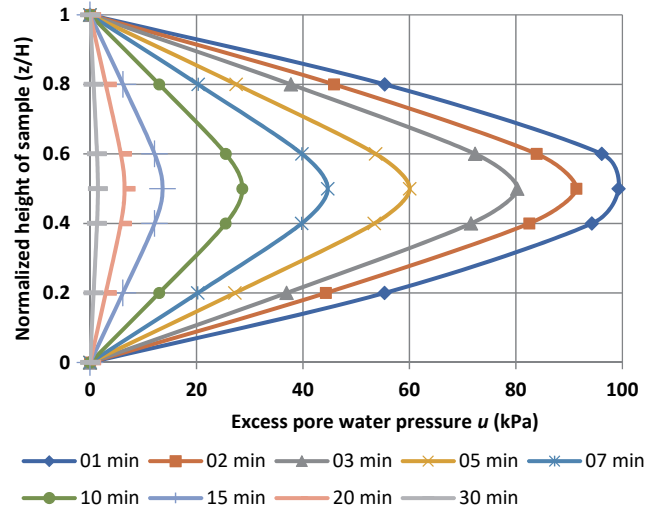


Fig. 2 Pore water pressure distribution along the soil sample versus time

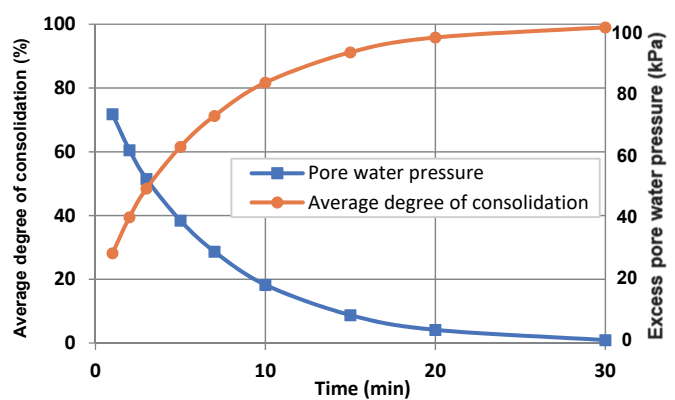


Fig. 3 Variation of average degree of consolidation and average pore water pressure versus time

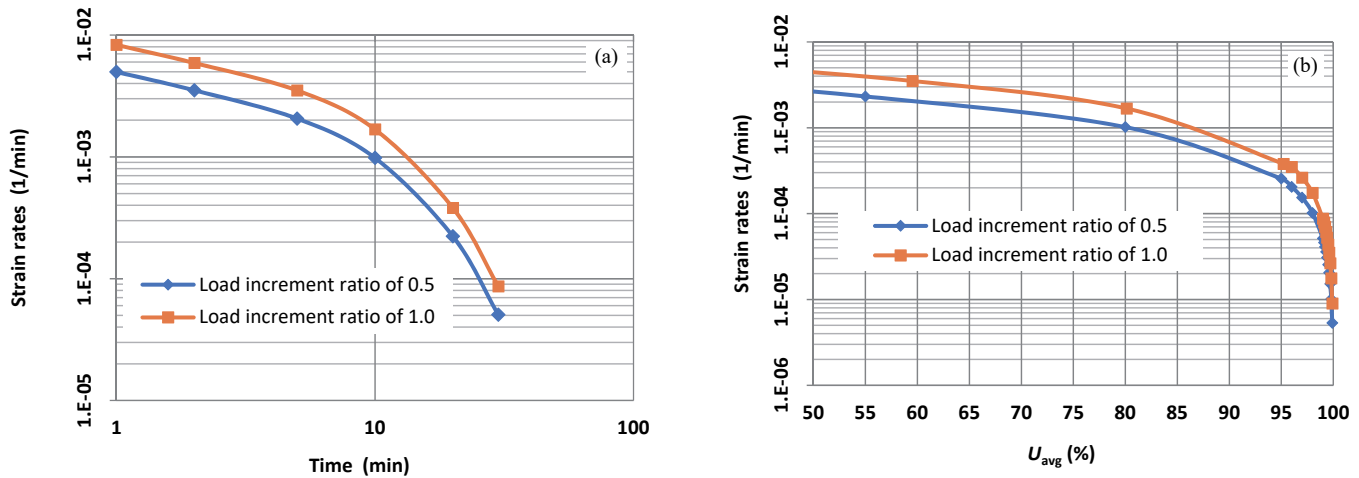


Fig. 4 Variation of estimated strain rates versus (a) time and (b) degree of consolidation for two values of load increment ratio

Moreover, the predicted strain rates at the end of the primary consolidation stage (at $U_{avg} = 99\%$ for example, noted $r_{99\%}$) were dependent on the applied loads. Figure 5 shows the increase in the predicted strain rate $r_{99\%}$ obtained by increasing the applied loads according to two load increment ratio values (0.5 and 1). It was observed that $r_{99\%}$ increased by approximately three to four times from the load of 15 kPa to the load of 1900 kPa. This was in good agreement with the experimental results obtained by Feng (2010) when the end-of-primary strain rate r_{cop} increased by two to three times from a load of 132 kPa to a maximum load of 1754 kPa, for different conventional oedometer tests.

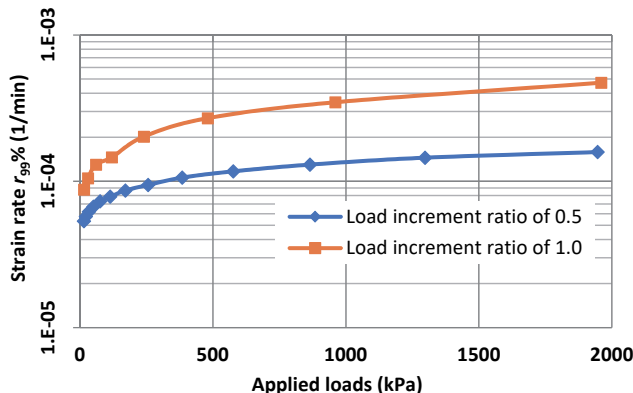


Fig. 5 Variation of estimated strain rate ($r_{99\%}$) versus applied loads for two values of load increment ratio

4. EXPERIMENTAL VERIFICATION OF NUMERICAL MODEL

To determine the capability of the developed numerical model to produce reliable primary consolidation strain rates, the results of the conventional oedometer tests conducted by Feng (2010) were used. The tests were carried out on four Kaolin samples prepared in a laboratory using a consolidometer measuring 20 cm in diameter and 6 cm in height. The samples were preloaded to 132 kPa in the consolidometer before being unloaded in steps to 0 kPa, after which they were extruded out and cut into different pieces. Two conventional oedometer tests were carried out on undisturbed samples (called tests C1 and C2) with different load

increment ratio values, while two other tests were carried out on disturbed samples (called tests C3 and C4) with different degrees of disturbance. The fundamental results of these tests are illustrated in the appendix at the end of this paper.

The $\epsilon_v - \log t$ curves obtained during the experimental tests were used to evaluate the experimental strain rate variations during each load increment using the following equations:

$$\text{For } t < t_p \quad r = 0.434 C_{re}/t \quad (16)$$

$$\text{For } t \geq t_p \quad r = 0.434 C_{ae}/t \quad (17)$$

where t_p is the time at the end of the primary consolidation. C_{re} and C_{ae} are the slopes of the $\epsilon_v - \log t$ curve before and after t_p , respectively.

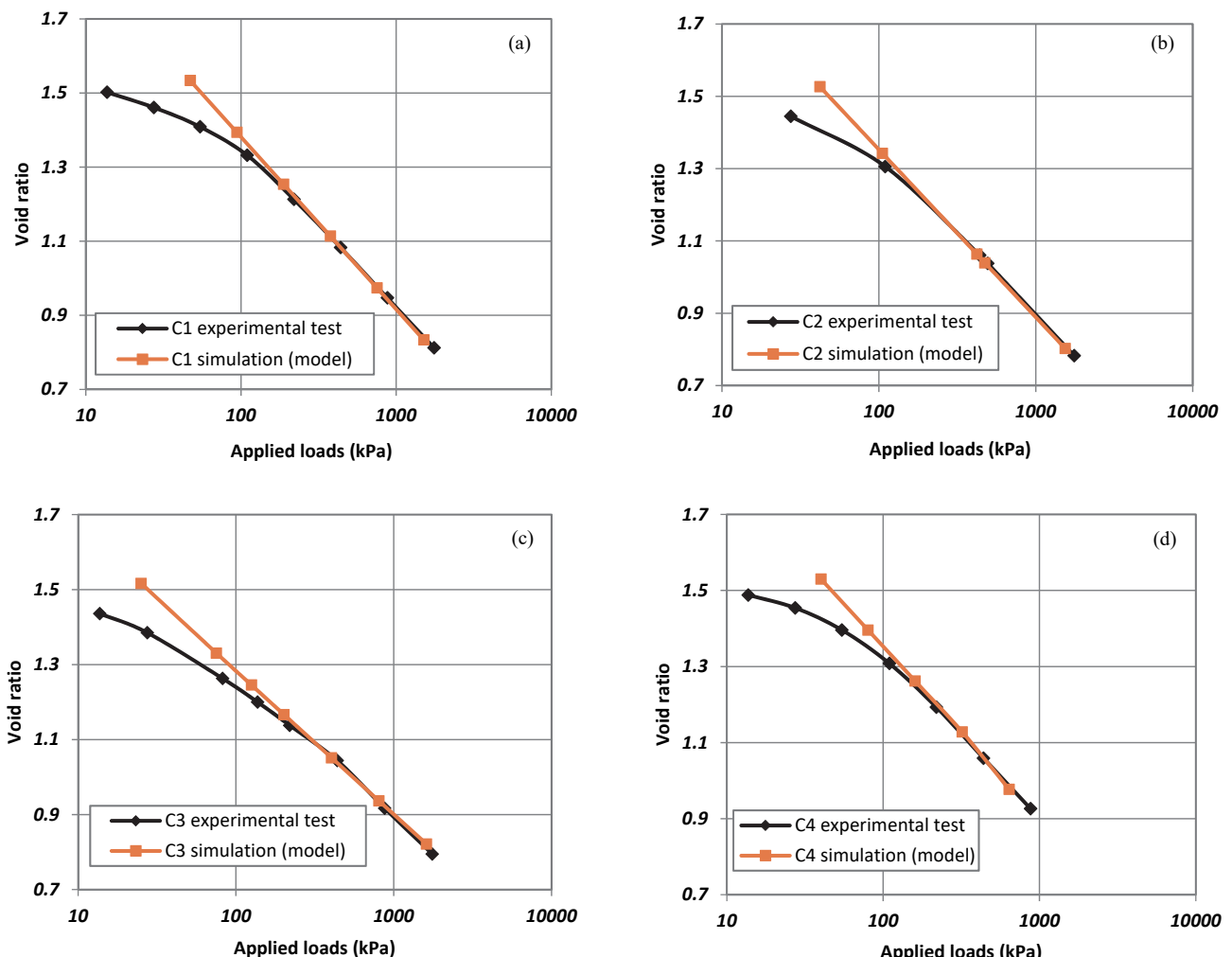
The two parameters of consolidation, c_v and C_c , obtained during each experimental test were used to evaluate the predicted strain rate variations using the developed model. Table 1 summarizes the characteristics used in different simulations of all the conventional oedometer tests.

Because the tested soil was overconsolidated, the numerical model was used to evaluate the predicted strain rate variations only in the virgin compression part for different oedometer tests. The applied loads during each simulation of the different oedometer tests were evaluated from the initial effective stress (which corresponds to e_0) by applying the same load increment ratio values adopted in the experimental tests (Fig. 6).

Figures 7 to 10 show the comparisons between the experimental and predicted strain rate variations for the different tests during the full duration of primary consolidation and only at the end of primary consolidation. The comparisons were conducted practically for the same range of applied loads, which varied from 109 kPa to 1753 kPa in the experimental case and from 75 kPa to 1600 kPa in the numerical case. Furthermore, each comparison is conducted between the strain rate variations under a given applied load during the experimental test (denoted E for the experimental case) and the predicted strain rate variations under the nearest load from the simulation of the same experimental test (denoted P for the predicted case). For example, the comparisons for test C1 were conducted between the loads of 109 kPa (E), 219 kPa (E), 438 kPa (E), 878 kPa (E), 1753 kPa (E) and the loads of 94 kPa (P), 188 kPa (P), 376 kPa (P), 752 kPa (P), 1504 kPa (P), respectively.

Table 1 Characteristics used for simulations of different tests

Test	Load increment	Load increment ratio	Applied loads (kPa)	H_i (cm)	H_{i+1} (cm)	e_i	e_{i+1}	c_v (cm ² /min)	c_c	n
C1	0	—	47	—	2.000	—	1.534	—	—	—
	1	1.0	94	2.000	1.889	1.534	1.394	0.0862	0.463	50
	2	1.0	188	1.889	1.779	1.394	1.254	0.0836	0.463	50
	3	1.0	376	1.779	1.668	1.254	1.114	0.1010	0.463	50
	4	1.0	752	1.668	1.557	1.114	0.974	0.1130	0.463	50
	5	1.0	1504	1.557	1.446	0.974	0.834	0.1240	0.463	50
C2	0	—	42	—	2.000	—	1.527	—	—	—
	1	1.5	105	2.000	1.854	1.527	1.343	0.0751	0.462	50
	2	3.0	420	1.854	1.634	1.343	1.064	0.0897	0.462	50
	3	0.125	472.5	1.634	1.615	1.064	1.040	0.0917	0.462	50
	4	2.25	1535.6	1.615	1.427	1.040	0.803	0.1060	0.462	50
C3	0	—	25	—	2.000	—	1.517	—	—	—
	1	2.0	75	2.000	1.855	1.517	1.331	0.0480	0.380	50
	2	0.667	125	1.855	1.788	1.331	1.246	0.0530	0.380	50
	3	0.607	200	1.788	1.725	1.246	1.167	0.0710	0.380	50
	4	1.0	400	1.725	1.633	1.167	1.052	0.0855	0.380	50
	5	1.0	800	1.633	1.541	1.052	0.937	0.0940	0.380	50
C4	0	—	40	—	2.000	—	1.530	—	—	—
	1	1.0	80	2.000	1.890	1.530	1.396	0.0750	0.443	50
	2	1.0	160	1.890	1.784	1.396	1.262	0.0780	0.443	50
	3	1.0	320	1.784	1.678	1.262	1.128	0.0810	0.443	50
	4	1.0	640	1.678	1.575	1.128	0.977	0.0840	0.443	50

**Fig. 6 Experimental and theoretical curves of compression used for evaluation of stain rates: (a) test C1; (b) test C2; (c) test C3; and (d) test C4**

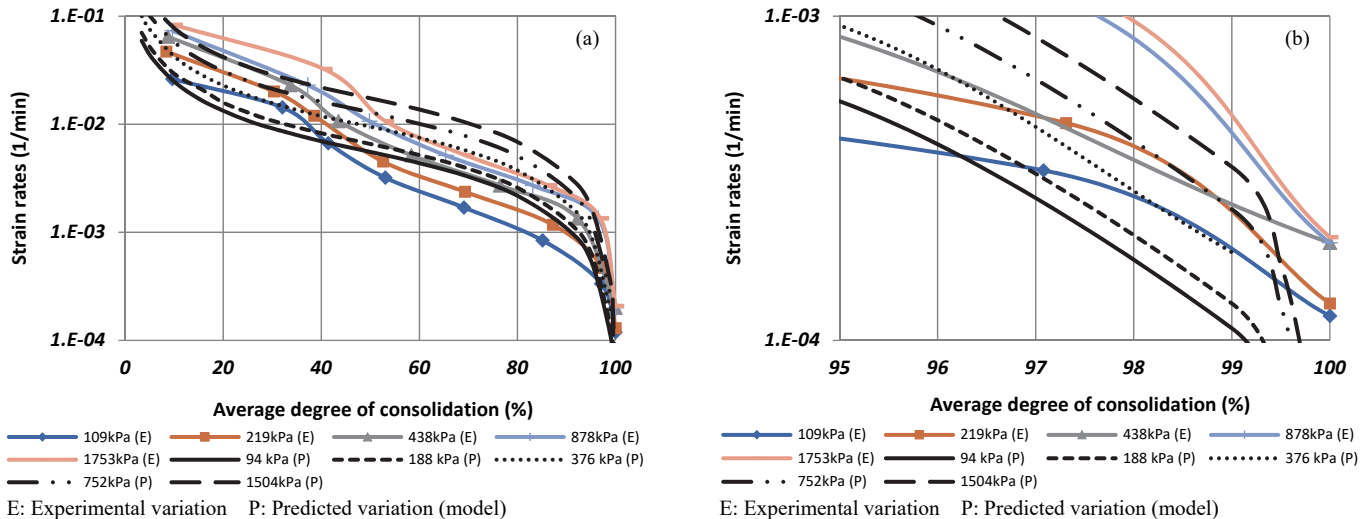


Fig. 7 Comparison between experimental and predicted variations of strain rate for test C1: (a) during all duration of primary consolidation stage; (b) at the end of primary consolidation stage

Firstly, it was observed that the strain rates decreased with the average degree of consolidation progress for both the experimental and predicted strain rate variations. Furthermore, a good convergence was obtained between the experimental and predicted strain rate variations, with very small differences that did not generally exceed twice the strain rates. For example, the comparison between the 109 kPa (E) case and 94 kPa (P) case for test C1 revealed that for $U_{\text{avg}} \leq 40\%$ the experimental strain rates varied between 2.62×10^{-2} 1/min at $U_{\text{avg}} = 10\%$ and 1.43×10^{-2} 1/min at $U_{\text{avg}} = 30\%$, while the predicted strain rates varied between 2.48×10^{-2} 1/min at $U_{\text{avg}} = 10\%$ and 9.2×10^{-3} 1/min at $U_{\text{avg}} = 30\%$. For $U_{\text{avg}} > 40\%$ the experimental strain rates varied between 3.5×10^{-3} 1/min at $U_{\text{avg}} = 50\%$ and 6.3×10^{-4} 1/min at $U_{\text{avg}} = 90\%$, while the predicted strain rates varied between 5.55×10^{-3} 1/min at $U_{\text{avg}} = 50\%$ and 1.09×10^{-3} 1/min at $U_{\text{avg}} = 90\%$. However, at the last stage of primary consolidation ($U_{\text{avg}} > 95\%$), the predicted strain rates rapidly decreased due to the very small strain in this phase. In contrast, the experimental strain rates varied but decreased less, which was due to the presence of secondary compression during the experimental tests.

Figure 11 summarizes the variations of strain rates at the end of the primary consolidation stage, as illustrated in Figs. 7(b) to

10(b). The end-of-primary strain rates (r_{eop}) obtained during the experimental tests corresponded to those obtained from the numerical simulations of these tests using the developed model, with the range of U_{avg} generally varying between 97.5% and 99.5%. This range of U_{avg} was situated at the end of the primary consolidation stage, indicating that the numerical model provided good end-of-primary strain rates. Besides, Lee *et al.* (1993) found that the appropriate strain rates for CRS consolidation tests conducted on undisturbed soil samples of Rio de Janeiro soft clays corresponded to those calculated when conventional oedometer tests were conducted on the same soil, with the range of U_{avg} varying between 80% and 95%. Then, if the end-of-primary strain rates obtained by Feng (which generally varied between 1×10^{-4} 1/min and 3×10^{-4} 1/min) were increased by 10 times to obtain the appropriate strain rates for the CRS test according to the Mesri and Feng criterion, the obtained strain rates (which varied between 1×10^{-3} 1/min and 3×10^{-3} 1/min) would correspond to those predicted by the numerical model when the range of U_{avg} generally varied between 75% and 95% (Figs. 7 to 10). This was in good agreement with the experimental results obtained by Lee *et al.* (1993).

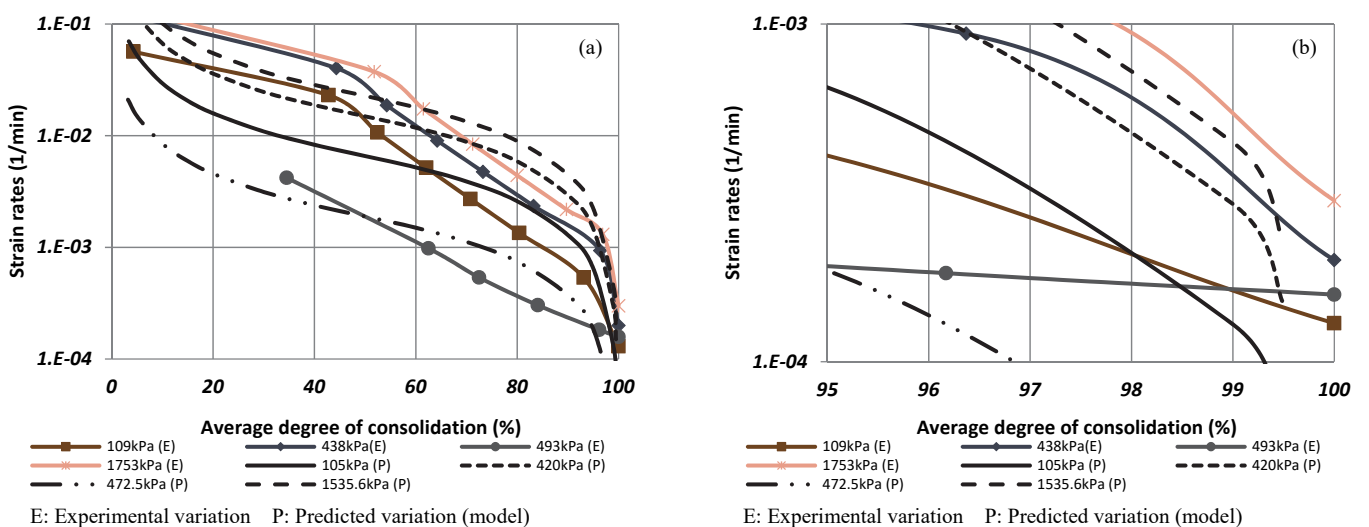


Fig. 8 Comparison between experimental and predicted variations of strain rate for test C2: (a) during all duration of primary consolidation stage; (b) at the end of primary consolidation stage

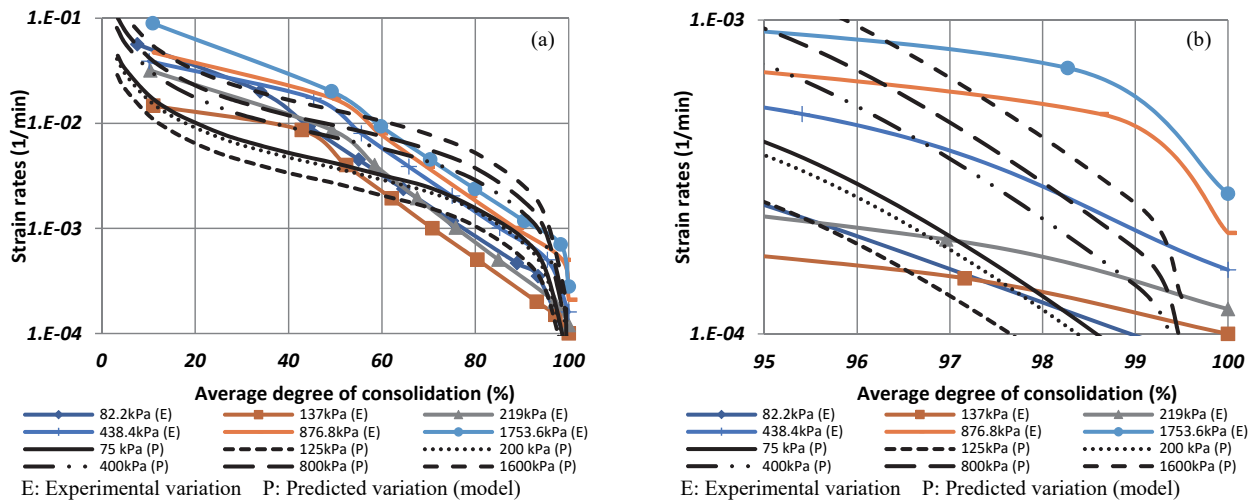


Fig. 9 Comparison between experimental and predicted variations of strain rate for test C3: (a) during all duration of primary consolidation stage; (b) at the end of primary consolidation stage

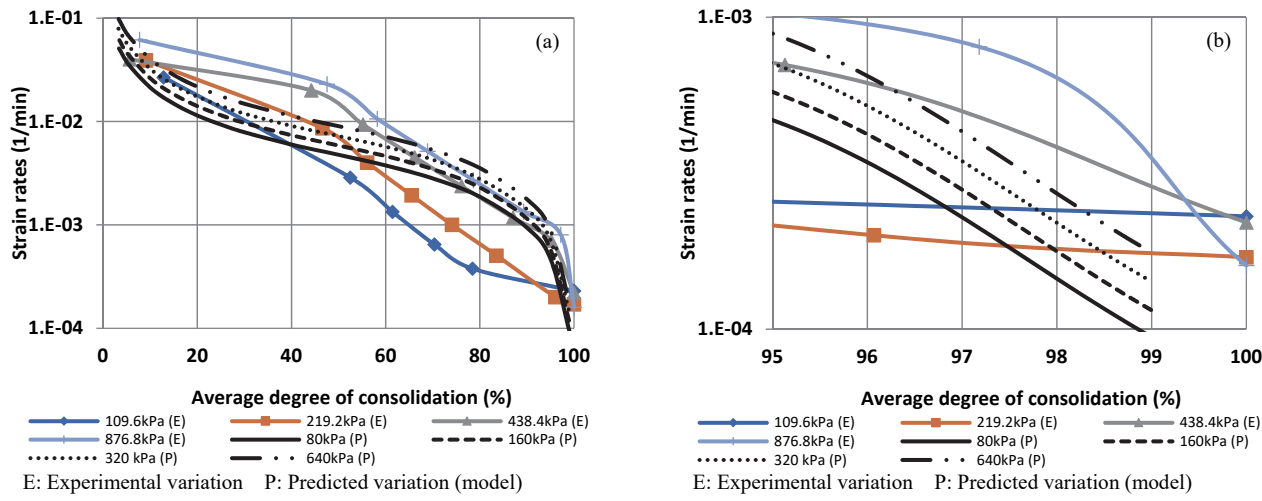


Fig. 10 Comparison between experimental and predicted variations of strain rate for test C4: (a) during all duration of primary consolidation stage; (b) at the end of primary consolidation stage

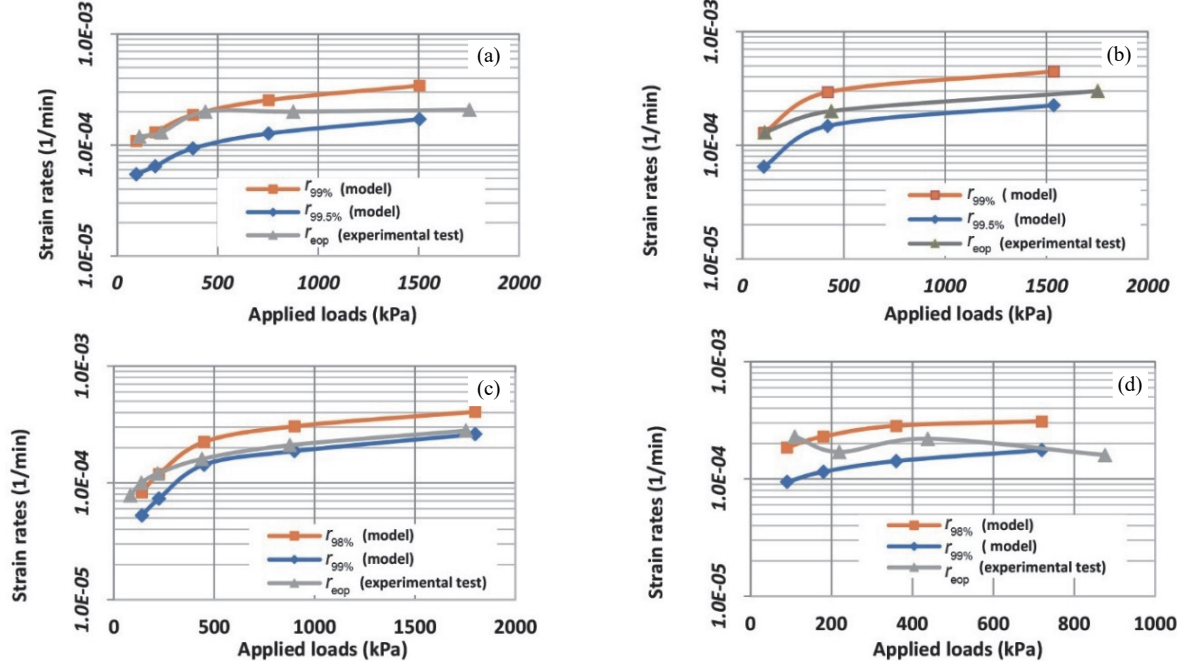


Fig. 11 Comparison between experimental and predicted strain rates at the end of primary consolidation: (a) test C1; (b) test C2; (c) test C3; and (d) test C4

Figure 12 shows the values of the average degree of consolidation at which the predicted strain rates corresponded exactly to the experimental end-of-primary strain rates evaluated during each load increment. These values varied between 97.5% and 99.5% for small applied loads, and between 98.5% and 99.5% for large applied loads. For more than 15 load increments for all the tests, the average value of all U_{avg} was practically 98.75%. Therefore, approximate end-of-primary strain rate values (r_{eop}) during the different load increments of the conventional oedometer test could be estimated using the developed model at a value of $U_{\text{avg}} \approx 99\%$, after which they could be used to evaluate the appropriate strain rates for the CRS test.

When using the numerical model to estimate appropriate strain rates for the CRS test, it would be necessary before conducting the tests to evaluate the initial height of the soil sample, H_0 , its initial void ratio, e_0 , the initial effective stress, σ_{v0} , and the Atterberg limits (to predict c_v and C_c). The obtained end-of-primary

strain rates depend strongly on the values of the consolidation characteristics (C_c and c_v) that can be estimated through correlations with the index properties of the tested soil. However, since the principal purpose of developing the numerical model was to give an approximate estimation of an appropriate margin of strain rates for the CRS test from the end-of-primary strain rates evaluated during a conventional oedometer test, a difference of two to three times between the estimated and measured strain rates was considered as acceptable. This was because the difference between the smallest and largest appropriate strain rates of the CRS test can sometimes exceed five times.

For example, the U.S Navy's approximate correlation between c_v and LL (Fig. 1) and the correlation between C_c and LL developed by Terzaghi and Peck (Eq. (11)) were used in this last part to study the difference that could be produced between the experimental end-of-primary strain rates (r_{eop}) and the predicted strain rates ($r_{99\%}$) for the undisturbed soil samples C1 and C2. The comparison was made in the virgin compression part using the same experimental load increment ratio values to obtain the successive applied loads during each test. The simulated strain rates ($r_{99\%}$) during each load increment for the two tests are listed in Table 2.

The comparison between the experimental end-of-primary strain rates (r_{eop}) and the predicted strain rates ($r_{99\%}$) is shown in Fig. 13. A small difference between the two types of strain rates (experimental and predicted) that does not exceed generally two times was observed for test C1, while a good agreement was observed for test C2, with the only exception being due to the very small load increment ratio of 0.125 adopted between the applied loads of 540 kPa and 608 kPa. It is noted that the use of general correlations for the undisturbed samples in this example led to an acceptable difference, but the selection of more particular correlations with respect to other parameters (nature of soil and region) might significantly reduce the difference.

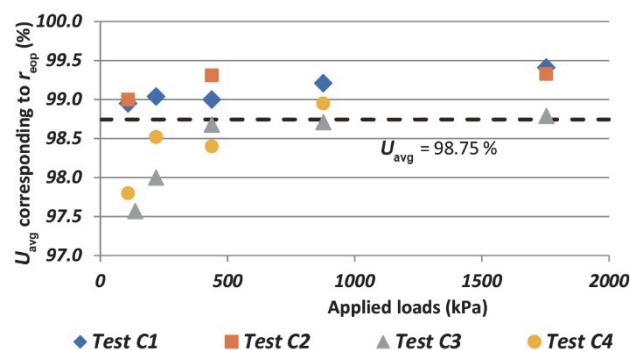


Fig. 12 Values of U_{avg} at which predicted strain rate equals to experimental r_{eop} for all load increments

Table 2 Characteristics used to simulate $r_{99\%}$ for tests C1 and C2

Test	Load increment	Load increment ratio	Applied loads (kPa)	H_i (cm)	H_{i+1} (cm)	e_i	e_{i+1}	c_v (cm ² /min)	C_c	$r_{99\%}$ (1/min)
C1	0	–	57	–	2.000	–	1.534	–	–	–
	1	1.0	114	2.000	1.859	1.534	1.355	0.030	0.594	5.03×10^{-5}
	2	1.0	228	1.859	1.718	1.355	1.176	0.030	0.594	6.25×10^{-5}
	3	1.0	456	1.718	1.577	1.176	0.998	0.030	0.594	7.94×10^{-5}
	4	1.0	912	1.577	1.435	0.998	0.819	0.030	0.594	1.02×10^{-4}
	5	1.0	1824	1.435	1.294	0.819	0.640	0.030	0.594	1.36×10^{-4}
C2	0	–	54	–	2.000	–	1.527	–	–	–
	1	1.5	135	2.000	1.813	1.527	1.291	0.030	0.594	6.68×10^{-5}
	2	3.0	540	1.813	1.530	1.291	0.933	0.030	0.594	1.35×10^{-4}
	3	0.125	608	1.530	1.506	0.933	0.903	0.030	0.594	1.91×10^{-5}
	4	2.25	1974	1.506	1.265	0.903	0.599	0.030	0.594	2.01×10^{-4}

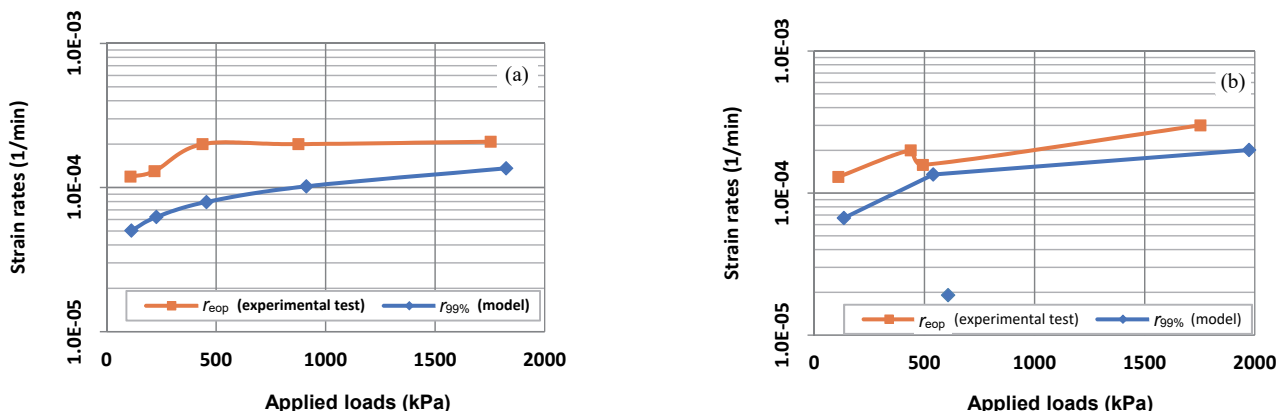


Fig. 13 Simulated strain rates ($r_{99\%}$) for (a) test C1 and (b) test C2

5. CONCLUSIONS

A numerical model based on the finite differences technique was developed in this work to predict the variations of strain rates during the primary consolidation stage for conventional oedometer tests. From the results of the numerical model, the following can be deduced:

1. The good accuracy of the developed model can be justified by the small difference obtained between the experimental strain rate variations evaluated from the conventional oedometer tests found in the literature and the strain rate variations predicted by a numerical simulation of the same tests.
2. The end-of-primary strain rates evaluated during the experimental tests corresponded to those predicted by the numerical simulation of the same tests, with the range of U_{avg} varying between 97.5% and 99.5% for small applied loads, and between 98.5% and 99.5% for large applied loads. A strain rate predicted at a value of $U_{avg} \approx 99\%$ by the numerical model could then be considered an end-of-primary strain rate.
3. Based on empirical correlations between the consolidation characteristics (c_v and C_c) and the index properties of the tested soil, an approximate estimation of the appropriate strain rates for the CRS test could be established from the predicted end-of-primary strain rate.

ACKNOWLEDGMENTS

The author acknowledges the reviewers and editors for providing guidelines to improve the quality of this paper.

FUNDING

The author received no funding for this work.

DATA AVAILABILITY

The data and/or computer codes used/generated in this study are available from the corresponding author on reasonable request.

CONFLICT OF INTEREST STATEMENT

There is no conflict of interest in this study.

REFERENCES

- Adams, A.L. (2011). *Laboratory Evaluation of the Constant Rate of Strain and Constant Head Techniques for Measurement of the Hydraulic Conductivity of Fine Grained Soils*. M.S. Thesis, Massachusetts Institute of Technology, Cambridge, MA. [http://www-udc.ig.utexas.edu/geofluids/Theses/Adams_thesis.pdf](http://www-udc.ig.utexas.edu/geofluids/Theeses/Adams_thesis.pdf)
- Ahmadi, H., Rahimi, H., Soroush, A., and Claes, A. (2014). "Experimental research on variation of pore water pressure in constant rate of strain consolidation test." *Acta Geotechnica Slovenica*, **2**, 47-57.
- Ahmadi, H., Hoofifar, A.H., Rahimi, H., and Soroush, A. (2009). "Hydraulic characteristics and pore water flow rule in constant rate of strain consolidation." *American Journal of Applied Sciences*, **6**(7), 1429-1435.
- <https://doi.org/10.3844/ajassp.2009.1429.1435>
- Almeida, M.S.S., Martins, I.S., and Carvalho, S.R.L. (1995). "Constant rate of strain consolidation of Singapore marine clay-discussion to paper: Lee K. et al. 1993." *Geotechnique*, **45**, 333-336. <https://doi.org/10.1680/geot.1995.45.2.333>
- ASTM D4186-12e1 (2012). *Standard Test Method for One-Dimensional Consolidation Properties of Saturated Cohesive Soils using Controlled-Strain Loading*. West Conshohocken, PA. <http://www.astm.org/Standards/D4186>
- ASTM D4186-06 (2006). *Standard Test Method for One-Dimensional Consolidation Properties of Saturated Cohesive Soils using Controlled-Strain Loading*. West Conshohocken, PA. <http://www.astm.org/Standards/D4186>
- Das, B.M. (2008). *Advanced Soil Mechanics*. 3th Ed., Taylor and Francis, London and New York, 300-310.
- Feng, T.W. (2010). "Some observations on the oedometric consolidation strain rate behaviors of saturated clay." *Journal of GeoEngineering*, **5**(1), 1-7.
- Fox, P.J., Pu, H., and Christian, J.T. (2014). "Evaluation of data analysis methods for the CRS consolidation test." *Journal of Geotechnics and Geoenvironmental Engineering*, ASCE, **140**(6), 04014020. [https://doi.org/10.1061/\(ASCE\)GT.1943-5606.0001103](https://doi.org/10.1061/(ASCE)GT.1943-5606.0001103)
- Gorman, C.T., Hopkins, T.C., Deen, R.C., and Drnevich, V.P. (1978). "Constant rate of strain and controlled gradient consolidation testing." *Geotechnical Testing Journal*, **1**(1), 3-15. <https://doi.org/10.1520/GTJ10363J>
- Kassim, K.A., Ahmad, S.A.R., Ahmad, B.H.K., Chong, S.Y., and Lam, C.S. (2016). "Criteria of acceptance for constant rate of strain consolidation test for tropical cohesive soil." *Geotechnical and Geological Engineering*, **34**(4), 931-947. <https://doi.org/10.1007/s10706-016-0016-8>
- Kaveh, D. and Şirin, Ö.İ. (2022). "A survey on the relationship between Compression index, coefficient of consolidation and Atterberg limits." *Journal of Sustainable Construction Materials and Technologies*, **7**(4), 302-315. <https://doi.org/10.47481/jscmt.1161504>
- Lee, K., Choa, V., Lee, S.H., and Quek, S.H. (1993). "Constant rate of strain consolidation of Singapore Marine Clay." *Geotechnique*, **43**(3), 471-488. <https://doi.org/10.1680/geot.1993.43.3.471>
- Lee, K. (1981). "Consolidation with constant rate of deformation." *Geotechnique*, **31**(2), 215-229. <https://doi.org/10.1680/geot.1981.31.2.215>
- Lee, K., and Sills, G.C. (1979). "A moving boundary approach to the large strain consolidation of a thin soil layer." *Proceedings of the 3rd International Conference on Numerical Methods in Geomechanics*, Rotterdam, 163-173.
- Leroueil, S., Kababji, M., Tavenas, F., and Bouchard, R. (1985). "Stress-strain-strain rate relation for the compressibility of sensitive natural clays." *Geotechnique*, **35**(2), 159-180. <https://doi.org/10.1680/geot.1985.35.2.159>
- Mesri, G. and Feng, T.W. (1992). "Constant rate of strain consolidation testing of soft clays." *Proceedings of the Marsal Symposium*, Mexico City, 49-59.
- Mieussens, C., Magnan, J.P., and Soyez, P. (1985). "Essais de compressibilité à l'oedomètre, Procédures recommandées par les laboratoires des ponts et chaussées." *Bulletin de liaison des laboratoires des ponts et chaussées*, N 139.
- Nasamatha, R. and Arumairaj, P.D. (2015). "Numerical modeling for prediction of compression index from soil index properties." *Electronic Journal of Geotechnical Engineering*, **20**, 4369-4378.
- Pu, H., Fox, P.J., and Liu, Y. (2013). "Model for large strain

- consolidation under constant rate of strain." *International Journal for Numerical and Analytical Methods in Geomechanics*, **37**(11), 1574-1590.
<https://doi.org/10.1002/nag.2100>
- Rashed, K.A., Salih, N.B., and Abdella, T.A. (2017). "Correlation of consistency and compressibility properties of soils in Sulaimani city." *Sulaimania Journal of Engineering Sciences*, **4**(5), 86-94.
- Rui, J., Jinchun, C., and Takenori, H. (2013). "Interpretation of coefficient of consolidation from CRS test results." *Geomechanics and Engineering*, **5**(1), 57-70.
<https://doi.org/10.12989/gae.2013.5.1.057>
- Sheahan, T.C. and Watters, P.J. (1997). "Experimental verification of CRS consolidation theory." *Journal of Geotechnical and Geoenvironmental Engineering*, ASCE, **123**(5), 430-437.
[https://doi.org/10.1061/\(ASCE\)1090-0241\(1997\)123:5\(430\)](https://doi.org/10.1061/(ASCE)1090-0241(1997)123:5(430))
- Smith, R.E. and Wahls, H.E. (1969). "Consolidation under constant rate of strain." *Journal of the Soil Mechanics and Foundations Division*, ASCE 95 (SM2), 519-539.
- Sridharan, A. and Nagaraj, H.B. (2004). "Coefficient of consolidation and its correlation with index properties of remolded soils." *Geotechnical Testing Journal*, **27**(5), 469-474.
<https://www.astm.org/gtj10784.html>
- Terzaghi, K. and Peck, R.B. (1967). *Soil Mechanics in Engineering Practice*. 2nd Ed., Wiley, New York.
- Tiwara, B. and Ajmera, B. (2012). "New correlation equations for compression index of remolded clays." *Journal of Geotechnical and Geoenvironmental Engineering*, ASCE, **138**(6), 757-762.
[https://doi.org/10.1061/\(ASCE\)GT.1943-5606.0000639](https://doi.org/10.1061/(ASCE)GT.1943-5606.0000639)
- U.S. NAVY. (1971). *Soil Mechanics, Foundations, and Earth Structures*. NAVFAC Design Manual DM-7, Washington, D.C.
- Vinod, P. and Bindu, J. (2010). "Compression index of highly plastic clays—An empirical correlation." *Indian Geotechnical Journal*, **40**(3), 174-180.
- Wissa, A.E.Z., Christian, J.T., Davis, E.H., and Heiberg, S. (1971). "Consolidation at constant rate of strain." *Journal of the Soil Mechanics and Foundations Division*, ASCE 97 (10), 1393-1413.
- Wroth, C.P. and Wood, D.M. (1978). "The correlation with index properties of some basic engineering properties of soils." *Canadian Geotechnical Journal*, **15**(2), 137-145.

APPENDIX

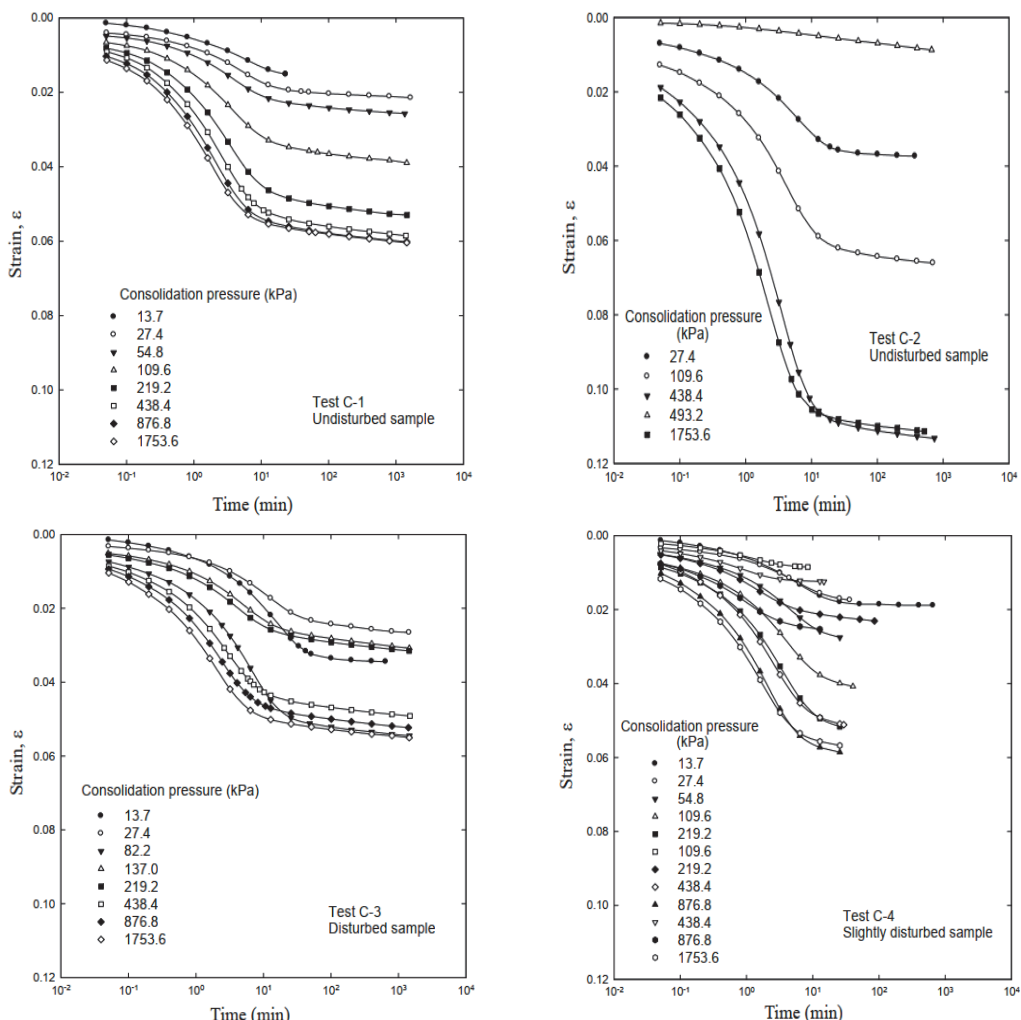


Fig. A1 Variations of measured strain ϵ versus time for tests C1 to C4 (Feng 2010)

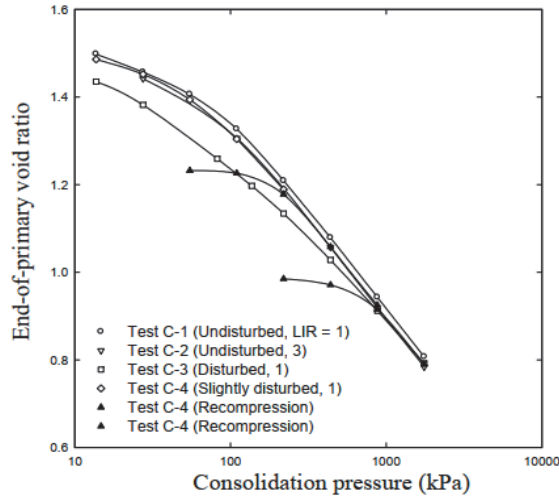


Fig. A2 End-of-primary compression curves for tests C1 to C4 (Feng 2010)

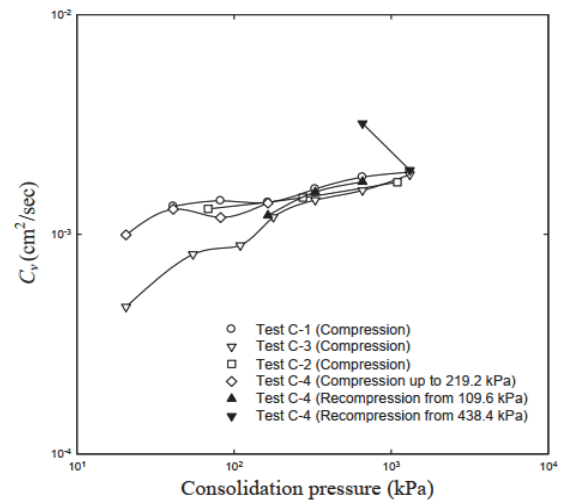


Fig. A3 Variations of coefficient of consolidation c_v with the applied pressures for tests C1 to C4 (Feng 2010)

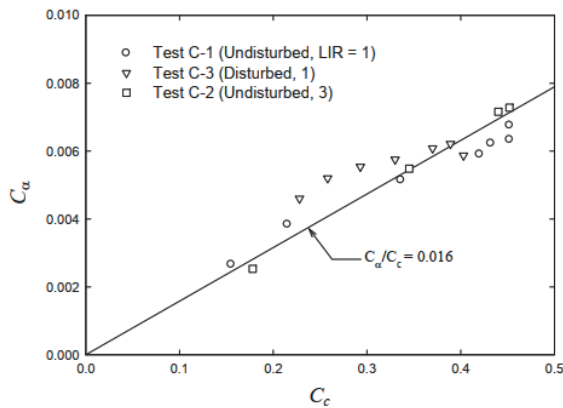


Fig. A4 Relationship between C_a and C_c for the Kaolin samples (Feng 2010)

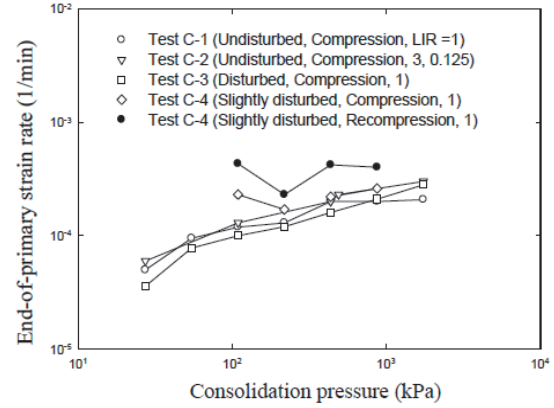


Fig. A5 Relationships between end-of-primary strain rate r_{eop} and the applied pressures (Feng 2010)